ORGANIC LETTERS

2013
Vol. 15, No. 6
1274–1277

A Novel Diketopyrrolopyrrole (DPP)-Based [2]Rotaxane for Highly Selective Optical Sensing of Fluoride

Mandapati V. Ramakrishnam Raju and Hong-Cheu Lin*

Department of Materials Science and Engineering, National Chiao Tung Univeristy, Hsinchu 30049, Taiwan (ROC)

linhc@mail.nctu.edu.tw

Received January 25, 2013

ABSTRACT

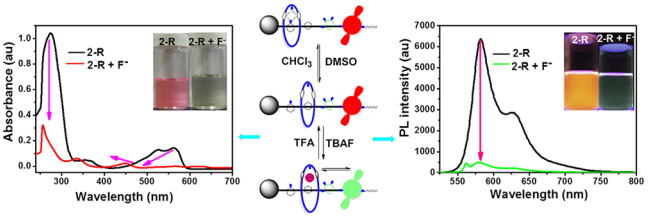

A novel [2]rotaxane based on an orthogonal H-bonded motif and 3,6-di(thiophen-2-yl)pyrrolo[3,4-*c*]pyrrole-1,4(2*H*,5*H*)-dione (DPP) with controlled topicity was successfully constructed, displaying excellent stimulated responses toward anion and solvent polarity. The preorganized host selectively recognized F^- with high optical sensitivity and reversibility via enhanced positive cooperativity and noncovalent interaction by evidence of a shorter fluorescence lifetime.

Developing bright and novel functional mechanically interlocked molecules (MIMs) with controlled topicity for selective and sensitive anion binding and sensing is of current research interest in the field of anion supramolecular chemistry owing to their indispensable roles in biological and chemical processes.[1] Due to its unique chemical properties and significant aspects in pharmacology, dental care, and treatment of osteoporosis, the fluoride ion is one of the most intriguing targets among all anions.[2] It is thus imperative to develop MIM based probes for sensitive and selective sensing of fluoride. Controlled topology has been elegantly utilized by nature in the recognition of anionic guests, inspired by many artificial anion receptors to be developed for the specific recognition of halides and other anions.[3] Myriads of molecular switches have been reported, due to their exquisite responsiveness to stimuli[4] and the handful of optical anion sensors;[5] however, those switches often suffered in the recognition of anionic guests in a discriminative fashion. To mimic this, we need a robust signaling unit (fluorophore) and a cavity with unique topological constraints formed in situ by virtue of mechanical bonding. Additionally pervasive advantages of chromogenic and fluorogenic molecular switches have been found because of their ease in responding to subtle guest interactions in microenvironments to perceivable outputs.[6]

(1) (a) Lehn, J.-M. *Supramolecular Chemistry: Concepts and Perspectives*; Wiley-VCH: New York, 1995. (b) Schmidtchen, F. P.; Berger, M. *Chem. Rev.* **1997**, *97*, 1609. (c) *Supramolecular Chemistry of Anions*; Wiley-VCH: New York, 1997. (d) Martķnez-Máñez.; Sancenón, F. *Chem. Rev.* **2003**, *103*, 4419.

(2) (a) Weatherall, A. *Pharmacology of Fluorides in Handbook of Experimental Pharmacology XX/1*, Part 1, Springer: Berlin, 1969; p 141. (b) Kirk, K. L. *Biochemistry of the Halogens and Inorganichalides*; Plenum: New York, 1991; p 58.

(3) (a) Pflugrath, J. W.; Quiocho, F. A. *Nature* **1985**, *314*, 257. (b) Sessler, J. L.; Camiolo, S.; Gale, P. A. *Coord. Chem. Rev.* **2003**, *240*, 17.

(4) (a) Altieri, A.; Bottari, G.; Dehez, F.; Leigh, D. A.; Wong, J. K. Y.; Zerbetto, F. *Angew. Chem., Int. Ed.* **2003**, *42*, 2296. (b) Qu, D. H.; Wang, Q. C.; Ren, J.; Tian, H. *Org. Lett.* **2004**, *6*, 2085. (c) Kwan, P. H.; MacLachlan, M. J.; Swager, T. M. *J. Am. Chem. Soc.* **2004**, *126*, 8638. (d) Onagi, H.; Rebek, J., Jr. *Chem. Commun.* **2005**, 4604. (e) Li, Y.; Li, H.; Li, Y.; Liu, H.; Wang, S.; He, X.; Wang, N.; Zhu, D. *Org. Lett.* **2005**, *7*, 4835. (f) Lankshear, M. D.; Beer, P. D. *Acc. Chem. Res.* **2007**, *40*, 657. (g) Lin, C.-F.; Liu, Y.-H.; Peng, S.-M.; Lai, C.-C.; Chiu, S.-H. *Chem.—Eur. J.* **2007**, *13*, 4350. (h) Zhou, W.-D.; Li, J.-B.; He, X.-R.; Li, C.-H.; Lv, J.; Li, Y.-L.; Wang, S.; Liu, H.-B.; Zhu, D.-B. *Chem.—Eur. J.* **2008**, *14*, 754. (i) Jiang, Q.; Zhang, H. Y.; Han, M.; Ding, Z. J.; Liu, Y. *Org. Lett.* **2010**, *12*, 1728. (j) Megiatto, J. D.; Schuster, D. I. *Org. Lett.* **2011**, *13*, 1808. (k) Li, H.; Zhang, H.; Zhang, Q.; Qu, D.-H. *Org. Lett.* **2012**, *14*, 5900.

(5) (a) Huang, Y.-L.; Hung, W.-C.; Lai, C.-C.; Liu, Y.-H.; Peng, S.-M.; Chiu, S.-H. *Angew. Chem., Int. Ed.* **2007**, *46*, 6629. (b) Lin, T.-Z.; Lai, C.-C.; Chiu, S.-H. *Org. Lett.* **2009**, *11*, 613. (c) Gassensmith, J. J.; Mattthys, S.; Lee, J.-J.; Wojcik, A.; Kamat, P. V.; Smith, B. D. *Chem.—Eur. J.* **2010**, *16*, 2916. (d) Evans, N. H.; Serpell, C. J.; Beer, P. D. *Chem. Commun.* **2011**, *47*, 8775. (e) Zhang, H.; Hu, J.; Qu, D.-H. *Org. Lett.* **2012**, *14*, 2334.

10.1021/ol400221h
Published on Web 03/05/2013

The exceptional thermal and light stabilities of 3,6-di(thiophen-2-yl)pyrrolo[3,4-*c*]pyrrole-1,4(2*H*,5*H*)-dione (DPP) and its derivatives along with the remarkable photophysical properties make them expedient candidates in designing new functional MIMs.[7] Since fluoride ions have a strong reactivity with receptor groups, such as amine, amide, lactam, urea, thiourea, and phenol, due to its high electronegativity and small ionic size, miscellaneous macrocyclic and tweezer-shaped receptors have been reported.[8] However, reports based on [2]rotaxanes with controllable topology under external stimuli that have specific anionic guest binding abilities are still due.

Herein, we designed and synthesized a first example of a DPP stoppered [2]rotaxane **2-P** containing an orthogonal bifurcated pyridine−pyridine H-bonded motif. This design was found to be ideal for solvent induced shuttling and specific fluoride ion sensing with sensitive chromogenic and fluorogenic functions along with remarkable reversibilities.[5a,9] The key building blocks, i.e., pseudorotaxane **2** and asymmetric diketopyrrolopyrrole derivative **3**, were prepared in good yields. Compound **2** was synthesized from the monodentate thread **1** and a preformed macrocycle-Pd tridentate ligand[10] using a palladium active metal template approach (see Supporting Scheme S1). Novel asymmetric DPP derivative **3** was prepared from **11** in three steps. First, compound **11** was monoalkylated with 2-ethylhexyl bromide to acquire compound **12**, which was further alkylated with propargyl bromide to afford **13**. Then, it was brominated by NBS to obtain asymmetric DPP derivative **3** as shown in Supporting Scheme S1.

The building blocks **2** and **3** were coupled by utilizing a click reaction strategy to afford metalated [2]rotaxane **2-M**, likewise the control axle **1-C** was prepared. To manipulate guest binding capabilities, **2-M** was demetalated using potassium cyanide in $CHCl_3$/MeOH to produce the final [2]rotaxane **2-P** as depicted in Scheme 1.

The ^{1}H NMR spectra of [2]rotaxane **2-P**, control axle **1-C**, and macrocycle were compared in $CDCl_3$ (Figure 1). Upfield shifts for axle pyridyl protons (12, 13, and 14) and macrocycle protons (E and F) along with a 1.5 ppm downfield shift for macrocycle amide protons C indicated

Scheme 1. Synthetic Route of [2]Rotaxane **2-P**

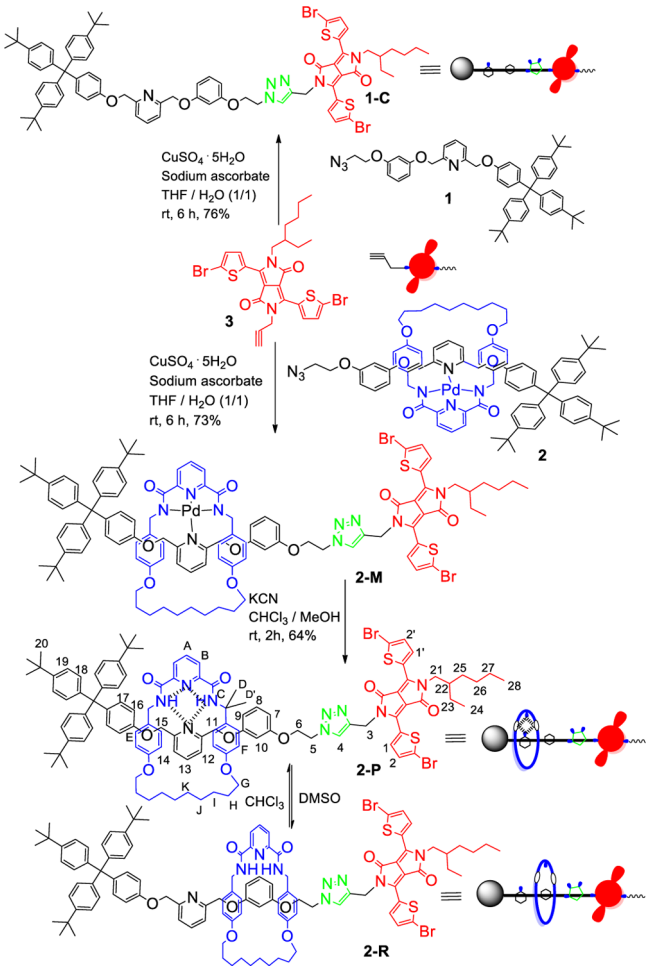

the existence of an overwhelming interlocked nature through an orthogonal bifurcated pyridine−pyridine H-bonding between axle and wheel. Moreover, in relatively polar solvent d_6-DMSO the observed upfield shifts for resorcinol protons (7 and 9) along with downfield shifts for pyridyl protons (12, 13, and 14) and macrocycle amide protons C suggested that the cycle was translocated to the resorcinol unit as the H-bonding basicity was increased (Scheme 1 and Figure 2). Thus, [2]rotaxane presents two translational isomers under different solvent polarities in which the macrocycle resides on the pyridine unit in $CDCl_3$ (translational isomer **2-P**) and on the resorcinol unit in DMSO (translational isomer **2-R**).[11]

To probe the anion recognition affinities of [2]rotaxane, we employed ^{1}H NMR titrations of **2-P** in $CDCl_3$ over a range of anions, such as F^-, Cl^-, Br^-, I^-, AcO^-, NO_3^-, and $H_2PO_4^-$, with 3 equiv of respective tetrabutylammonium salts (Figure S1). Interestingly, no other anions showed any significant spectroscopic changes except F^-. Taking this vivid spectroscopic clue, further titrations were conducted

(6) Lakowicz, J. R. *Principles of Fluorescence Spectroscopy*; Kluwer Academic/Plenum: New York, 1999.

(7) Hao, Z.; Iqbal, A. *Chem. Soc. Rev.* **1997**, *26*, 203.

(8) (a) Korendovych, I. V.; Cho, M.; Butler, P. L.; Stapless, R. J.; Rybak-Akimova, E. V. *Org. Lett.* **2006**, *8*, 3171. (b) Kaewtong, C.; Fuangswasdi, S.; Muangsin, N.; Chaichit, N.; Vicens, J.; Pulpoka, B. *Org. Lett.* **2006**, *8*, 1561. (c) Kim, J. S.; Quang, D. T. *Chem. Rev.* **2007**, *107*, 3780. (d) Sessler, J. L.; Kim, S. K.; Gross, D. E.; Lee, C. H.; Kim, J. S.; Lynch, V. M. *J. Am. Chem. Soc.* **2008**, *130*, 13162. (e) Kim, S. K.; Lynch, V.; Young, N. J.; Hay, B. P.; Lee, C. H.; Kim, J. S.; Moyer, B. A.; Sessler, J. L. *J. Am. Chem. Soc.* **2012**, *134*, 20837. (f) Thiampanya, P.; Muangsin, N.; Pulpoka, B. *Org. Lett.* **2012**, *14*, 4050.

(9) Barrell, M. J.; Leigh, D. A.; Lusby, P. J.; Slawin, A. M. Z. *Angew. Chem., Int. Ed.* **2008**, *47*, 8036.

(10) (a) Furusho, Y.; Matsuyama, T.; Takata, T.; Moriuchi, T.; Hirao, T. *Tetrahedron Lett.* **2004**, *45*, 9593. (b) Fuller, A. M.; Leigh, D. A.; Lusby, P. J.; Oswald, I. D. H.; Parsons, S.; Walker, D. B. *Angew. Chem., Int. Ed.* **2004**, *43*, 3914. (c) Leigh, D. A.; Lusby, P. J.; Slawin, A. M. Z.; Walker, D. B. *Angew. Chem., Int. Ed.* **2005**, *44*, 4557. (d) Crowley, J. D.; Leigh, D. A.; Lusby, P. J.; MaBurney, R. T.; Perret-Aebi, L.-E.; Petzold, C.; Slawin, A. M. Z.; Symes, M. D. *J. Am. Chem. Soc.* **2007**, *129*, 15085. (e) Fuller, A. M.; Leigh, D. A.; Lusby, P. J. *J. Am. Chem. Soc.* **2010**, *132*, 4954.

(11) (a) Lane, A. S.; Leigh, D. A.; Murphy, A. *J. Am. Chem. Soc.* **1997**, *119*, 11092. (b) Chiang, P.-T.; Cheng, P.-N.; Lin, C.-F.; Liu, Y.-H.; Lai, C.-C.; Peng, S.-M.; Chiu, S.-H. *Chem.—Eur. J.* **2006**, *12*, 865. (c) Mateo-Alonso, A.; Ehil, C.; Guldi, D. M.; Prato, M. *Org. Lett.* **2013**, *15*, 84.

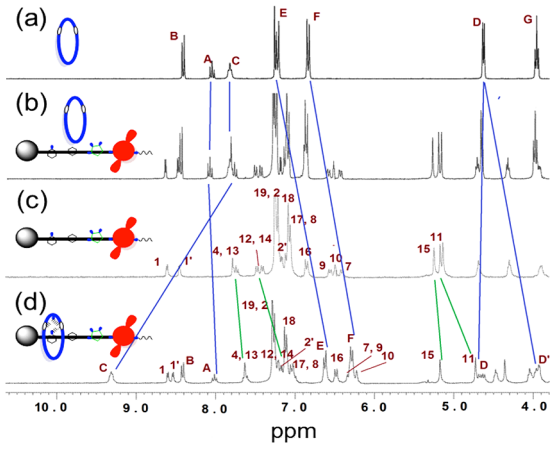

Figure 1. ^{1}H NMR spectra ($CDCl_3$, 300 MHz, 298 K): (a) macrocycle, (b) 1:1 mixture of control axle **1-C** and macrocycle, (c) **1-C**, (d) [2]rotaxane **2-P**. The assignments correspond to the lettering shown in Scheme 1 (numerical and alphabetical lettering indicating dumbbell part and macrocycle, respectively).

with F^-. Upon the progressive addition of F^-, significant upfield shifts were observed for cavity and thread protons along with the disappearance of amide NH protons at 1 equiv of F^-. On further addition, no obvious changes were observed as shown in Figure S2. Importantly, the [2]rotaxane precursors, such as **1-C** and **2-M**, could not show observable changes with the addition of 3 equiv of F^- (Figure S3).

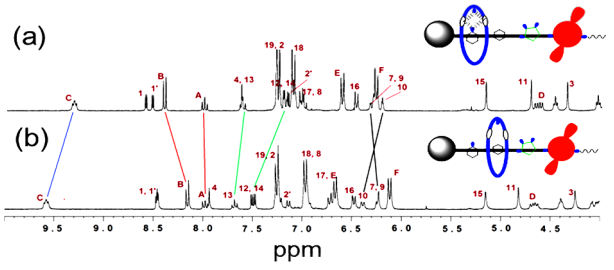

Figure 2. ^{1}H NMR spectra (300 MHz, 298 K): (a) [2]rotaxane translational isomer **2-P** in $CDCl_3$, (b) [2]rotaxane translational isomer **2-R** in d_6-DMSO. The assignments correspond to the lettering shown in Scheme 1.

Furthermore, ^{1}H and ^{19}F NMR titrations were conducted in polar solvent DMSO to appreciate the sensing ability of [2]rotaxane and to attain a better insight into the binding interaction of **2-R**/F^-. The ^{1}H NMR spectrum of **2-R** showed significant changes upon the addition of F^-. As the addition of F^- reached 1 equiv, the cavity and thread protons, such as pyridine and the resorcinol unit, showed upfield shifts. On further addition the spectrum became broad as well as the amide NH proton C completely disappeared and formed a strong HF_2^- peak at 4 equiv of F^- (Figure 3).

Delightfully, the binding mode was clearly revealed by ^{19}F NMR titrations in DMSO, in which the sharp singlet

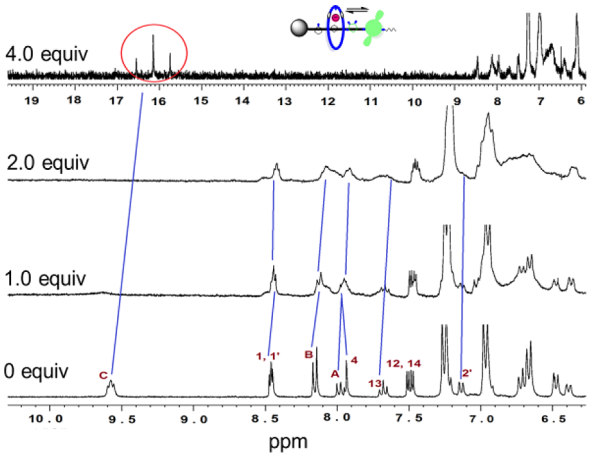

Figure 3. Changes in ^{1}H NMR (300 MHz, d_6-DMSO, 298 K) spectrum of [2]rotaxane **2-R** (3 mM) during titration with TBAF (0−4 equiv). Red circled region indicating the formation of the HF_2^- ion. The assignments correspond to the lettering shown in Scheme 1.

corresponding to free TBAF at −102.5 ppm was upfielded to −103.8 ppm ($\Delta\delta$ = 1.3 ppm) upon the addition of **2-R** solution (3 equiv) to TBAF. Moreover, the weak doublet corresponding to HF_2^- at −143.1 ppm was gradually raised in its intensity with a declined triplet intensity of DF_2^- at −143.5 ppm simultaneously as depicted in Figure S4.[8a] Importantly the binding process of **2-R**/F^- was completely reversible upon the addition of CF_3COOH (TFA, 5 equiv) and provided a spectrum identical to that of the original rotaxane (Figure S5). Thus, [2]rotaxane **2-R** selectively recognized F^- through a noncovalent interaction due to a positive cooperativity between the 2,6-dicarboxyamidopyridine receptor (in macrocycle) and F^-, and further guest equivalents would deprotonate the amide cleft and induce a macrocycle shuttling.

Next, we focused on the photophysical properties of **1-C**, **2-M**, and **2-R** under the influence of chemical stimuli (solvent and anionic guests). To escalate future aqueous soluble functional MIMs, we further carried out all photophysical measurements in DMSO. Both absorption and fluorescence intensities of [2]rotaxane were sharply decreased in the relative polar solvent DMSO (Figure S6), which lucidly indicated the translocation of the wheel from pyridine to the resorcinol unit as the H-bond formed between pyridine and the wheel was disrupted, which is consistent with our above ^{1}H NMR observations as well as previous reports.[4d,11c]

UV−vis and fluorescence measurements were explored to probe the optical anion sensing abilities of **2-R**, and significant absorption changes in the absorption maxima of DPP (564 and 525 nm) and nonfluorogenic axle part (274 nm) were observed. As depicted in Figure 4a, upon the gradual addition of TBAF (0−40 equiv), the original absorption maxima of DPP decreased with two emerging new peaks at 257 and 451 nm. Simultaneously, the emission maximum of **2-R** at 582 nm (λ_{ex} = 525 nm) was

gradually quenched (Figure 4b). Since the titration patterns of absorption and ^{1}H NMR were complex, we employed fluorescence titrations to determine the stoichiometry and binding constant. Unambiguously, the results established a 1:1 stoichiometry of the **2-R**/F^- complex and yielded a binding constant of 2.65×10^4 M^{-1} (see Figures S7a and S7b).[12,13]

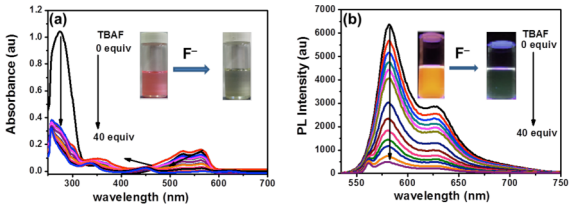

Figure 4. (a, b) UV−vis and fluorescence spectral changes of **2-R** (1×10^{-5} M in DMSO) upon the addition of TBAF in DMSO (0−40 equiv), respectively. Inset pictures in (a) and (b) indicate naked eye color changes as well as fluorescence changes under UV light (365 nm) upon the addition of TBAF, respectively (λ_{ex} = 525 nm).

Further selectivity of the [2]rotaxane host system was verified by titrations of anions, such as Cl^-, Br^-, I^-, AcO^-, NO_3^-, and $H_2PO_4^-$. Importantly, none of the above anions could show noticeable changes in either the absorption or emission spectra. Moreover, to strengthen the selectivity of [2]rotaxane, we did control titrations on its precursors **1-C** and **2-M**. However, their responses were trivial under similar conditions (see Figures S8a−S8f).

The observable naked eye color change of **2-R** from pink to pale green upon the addition of TBAF was consistent with our absorption trends. Other anions could not change the color, as their sizes were too large to interact with the cavity. Moreover, **1-C** and **2-M** did not show any obvious color changes with all anions (see Figures S9a−S9d). Remarkably, the on−off−on fluorescence etiquette of the **2-R**/F^- complex was successfully achieved via the alternative addition of F^- and TFA up to four cycles, which proved the excellent chromogenic and fluorogenic functions along with reversibility of this novel functional molecular switch. To verify the dramatic color change and fluorescence quenching of the DPP molecule, we further carried out electrochemical titrations of **2-P** with F^- (see Figures S10a and S10b). A dramatic cathodic shift of $\Delta E_{1/2}$ = 450 mv at 1 equiv of F^- was observed, and a further addition of F^- showed a steady cathodic perturbation, which is consistent with our ^{1}H NMR and UV−vis titration trends. Based on these results, we infer that the smallest anion F^- could be easily percolated into the macrocycle to form H-bonding with the 2,6-dicarboxyamidopyridine unit, and further guest equivalents would deprotonate the amide cleft to induce the shuttling of the charged wheel over the thread and to close the proximity of DPP in relative polar solvent DMSO. Eventually, this process facilitates the supramolecular electronic coupling between DPP and the **2-R**/F^- complex and thus affects the photophysical properties of the current functional MIM.[5d,14]

To corroborate the above observations, time-resolved fluorescence measurements were carried out for the **2-R** and **2-R**/F^- complex probed at 582 nm (excited at 525 nm). Significantly, as shown in Figure 5, time-resolved fluorescence became a biexponential decay with the lifetime of (τ_1) 5.71 ns (69.21%) and (τ_2) 2.19 ns (30.79%) from the original monoexponential decay with a lifetime of (τ_1) 5.56 ns. The shorter value can be attributed to the charged wheel (amide deprotonation by F^-), and the longer value represents the intrinsic fluorescence of the DPP fluorophore. However, the lifetime values of **1-C** and **2-M** remained constant from their original monoexponential decay even in the presence of F^- (see Figures S11a and S11b).

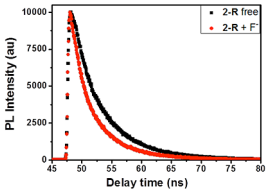

Figure 5. Time resolved fluorescence spectral changes of [2]rotaxane **2-R** before and after the addition of TBAF.

In summary, a bright DPP functionalized [2]rotaxane was synthesized and well characterized. The preorganized cavity formed in rotaxane by virtue of mechanical bond enhanced stimulated responses toward solvent and F^- via noncovalent interactions. It was demonstrated spectroscopically that the [2]rotaxane **2-R** host could selectively recognize F^- with remarkable chromogenic, fluorogenic, and reversible functions. A prevailing time-resolved fluorescence profile proved the sensitivity of **2-R** in contrast to its precursors. As the complex quenching mechanism was coupled with both charged macrocycle shuttling and chemical stimuli, the electron or energy transfer between macrocycle and fluorophore could not be easily differentiated. Further kinetic and transient absorption studies are currently underway in our laboratory, which will be reported in due course. Hence, this design of functional MIMs could be ideal for developing future allosteric anion sensors.

Acknowledgment. We thank the National Science Council of Taiwan (ROC) for financial support of this project through NSC 99-2113-M-009-006-MY2 and NSC 99-2221-E-009-008-MY2.

Supporting Information Available. Synthetic procedures, supporting Figures S1−S11, and compound characterization data (IR, ^{1}H, ^{13}C NMR, and MALDI-TOF mass). This material is available free of charge via the Internet at http://pubs.acs.org.

(12) Strutt, N. L.; Forgan, R. S.; Spruell, J. M.; Batros, Y. Y.; Stoddart, J. F. *J. Am. Chem. Soc.* **2011**, *133*, 5668.
(13) Connors, K. A. *Binding Constants*; Wiley: New York, 1987.
(14) Fukuzumi, S.; Ohukubo, K.; D'Souza, F.; Sessler, J. L. *Chem. Commun.* **2012**, *48*, 9801.

The authors declare no competing financial interest.